High-significance Sunyaev–Zel'dovich measurement: Abell 1914 seen with the Arcminute Microkelvin Imager

AMI Collaboration: Robert Barker,[1] Phillip Biddulph,[1] Dennis Bly,[1] Roger Boysen,[1] Anthony Brown,[1] Christopher Clementson,[1] Michael Crofts,[1] Thomas Culverhouse,[1] Jaroslaw Czeres,[1] Roger Dace,[1] Robert D'Alessandro,[1] Peter Doherty,[1] Peter Duffett-Smith,[1] Kenneth Duggan,[1] John Ely,[1] Mike Felvus,[1] William Flynn,[1] Jörn Geisbüsch,[1] Keith Grainge,[1][*] William Grainger,[2] David Hammet,[1] Richard Hills,[1] Michael Hobson,[1] Christian Holler,[1] Roy Jilley,[1] Michael E. Jones,[3] Takeshi Kaneko,[1] Rüdiger Kneissl,[4] Katy Lancaster,[5] Anthony Lasenby,[1] Phil Marshall,[6] Francis Newton,[1] Oliver Norris,[1] Ian Northrop,[1] Guy Pooley,[1] Vic Quy,[1] Richard D. E. Saunders,[1] Anna Scaife,[1] Jack Schofield,[1] Paul Scott,[1] Clive Shaw,[1] Angela C. Taylor,[3] David Titterington,[1] Marko Velić,[1] Elizabeth Waldram,[1] Simon West,[1] Brian Wood,[1] Ghassan Yassin,[3] Jonathan Zwart.[1]

[1] *Astrophysics Group, Cavendish Laboratory, University of Cambridge.*
[2] *Columbia University, New York, U.S.A.*
[3] *Astrophysics Group, Denys Wilkinson Building, Univerity of Oxford.*
[4] *Department of Astronomy, Department of Physics, 366 LeConte Hall, University of California, Berkeley, U.S.A.*
[5] *Astrophysics Group, HH Wills Physics Laboratory, Tyndall Avenue, Bristol.*
[6] *Kavli Institute for Particle Astrophysics and Cosmology, Stanford, U.S.A.*

ABSTRACT

We report the first detection of a Sunyaev–Zel'dovich (S–Z) decrement with the Arcminute Microkelvin Imager (AMI). We have made commissioning observations towards the cluster A1914 and have measured an integrated flux density of -8.61 mJy in a *uv*-tapered map with noise level 0.19 mJy/beam. We find that the spectrum of the decrement, measured in the six channels between 13.5–18 GHz, is consistent with that expected for a S–Z effect. The sensitivity of the telescope is consistent with the figures used in our simulations of cluster surveys with AMI.

Key words: cosmic microwave background – galaxies:clusters:individual (A1914)

1 INTRODUCTION

The Sunyaev–Zel'dovich effect (Sunyaev & Zel'dovich 1972) is a secondary anisotropy on the Cosmic Microwave Background (CMB) radiation due to inverse-Compton scattering of CMB photons from hot plasma in the gravitational potential of a cluster of galaxies. The S–Z effect has been detected by a number of different groups using a variety of observing techniques (e.g. Birkinshaw & Hughes 1994; Myers et al. 1997; Reese et al. 2000; Komatsu et al. 1999; Pointecouteau et al. 1999; Holzapfel et al. 1997; Grainge et al. 1993; Lancaster et al. 2005; Udomprasert et al. 2004. See e.g. Birkinshaw 1999 or Carlstrom et al. 2002 for a full review). For example, in the past, the Cambridge group used the five antennas of the Ryle Telescope (RT) in a compact configuration to produce S–Z maps such as that shown in Figure 1 (Jones et al. 2005). We detected a S–Z decrement towards the cluster A1914 with an integrated flux of -0.76 mJy and a map noise of 0.06 mJy/beam from a 228-hour observation. This long in-

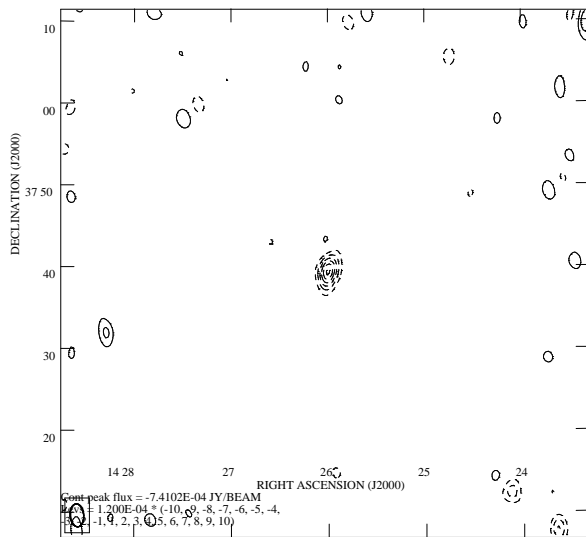[*] Issuing author – e-mail:kjbg1@mrao.cam.ac.uk

Figure 1. CLEANed RT map of the S–Z effect in A1914 after source subtraction. The integrated flux of the S–Z decrement is -0.76 mJy and the noise on the map is 0.06 mJy/beam. The field of view is chosen to be the same as that in Figures 2 and 5 for ease of comparison. In this and subsequent maps: dashed contours are negative, solid ones positive; the boxed ellipse in the lower left corner indicates the FWHM of the synthesised beam.

tegration time was required because the RT has relatively poor system temperature, has bandwidth of only 350 MHz and because the telescope baselines were long compared to the optimum required to match to the angular size of the cluster, with the result that most of the S–Z signal is resolved out.

The S–Z effect has the unique property that its surface brightness is independent of redshift. This makes it ideal as a means of surveying for galaxy clusters back to their epoch of formation. Several dedicated instruments are now being built to conduct such S–Z surveys (see e.g. Mohr et al 2000; Lo 2002; Mohr et al. 2003; Kosowsky 2003; Kneissl et al. 2001). At Cambridge, the Arcminute Microkelvin Imager (AMI) is being commissioned. This instrument has been designed to make high-speed, sensitive surveys for S–Z decrements by using many small dishes packed together in a compact array with a low noise, high-bandwidth back-end system and complemented by an array of much larger dishes designed to detect and subtract compact foreground radio sources. In this paper we present a commissioning observation with AMI towards A1914 which has previously been observed in S–Z (Grego et al. 2001; Jones et al. 2005) and in X-ray (see e.g. Ebeling et al. 1998; Böhringer et al. 2000; Ikebe et al. I2002).

2   THE ARCMINUTE MICROKELVIN IMAGER

AMI (Jones 2002) comprises two synthesis arrays, one of ten 3.7-m antennas (Small Array) and one of eight 13-m antennas (Large Array), both sited at Lord's Bridge, Cambridge.

The Large Array is an upgraded version of the RT, with the three outlying antennas now moved into a compact configuration near the five which we previously used for S–Z work. The telescope observes in the band 12–18 GHz with cryostatically cooled NRAO indium-phosphide front-end amplifiers. The overall system temperature is approximately 25 K. The radio frequency is mixed with a 24-GHz local oscillator, downconverting to an intermediate frequency (IF) band of 6–12 GHz. Amplification, equalisation, path compensation and automatic gain control are then applied to the IF signal. The correlator is an analogue Fourier transform spectrometer with 16 correlations formed for each baseline at path delays spaced by 25 mm. In addition, both '+' and '−' correlations are formed by use of $0°$ and $180°$ hybrids respectively. From these, eight 0.75-GHz channels are synthesised.

3   OBSERVATIONS

The new observations presented here are commissioning runs with just eight antennas of the Small Array and only the upper six frequency channels (giving a total of 4.5 GHz of bandwidth). We observed Abell 1914 for a total of 34 hours between 2005 August 15 and 2005 August 29 with a pointing centre of 14 26 02.15 +37 50 05.8 (J2000). The observations were phase and amplitude calibrated on 3C286. We take the flux density of 3C286 as 3.48 Jy (Baars et al. 1977) in $I + Q$ at 15 GHz with a spectrum of $\alpha = 0.733$ ($S \propto \nu^{-\alpha}$); a correction factor of 1.05 has been assumed to account for the $\approx 12\%$ polarisation at position angle $33°$ of the source. Specialist AMI data reduction software (the REDUCE package) was used to flag the data for telescope pointing errors, to excise interference, to apply the calibration and to weight the data. Reduced data were then transferred to AIPS for further analysis.

4   RESULTS

A naturally weighted map of the A1914 field is shown in Figure 2 and a plot showing the coverage of the aperture plane in Figure 3. The negative feature at the centre of the CLEANed map is the S–Z effect from the cluster, but it is confused by several radio sources which are also visible and whose effects must be subtracted. The brighter sources were mapped individually with the RT at the same frequency to determine their positions and fluxes. Contributions from sources close to the cluster centre were estimated from the 19-day RT observations (Section 1). Once these sources were removed, the AMI data were remapped and the fluxes of any remaining faint sources estimated and removed from the visibilities, a method we have found to be successful with previous RT S–Z observations (see e.g. Grainge et al. 1996). In all, 18 sources were subtracted from the visibility data as described in Table 1. The positions of the subtracted sources are shown on an NVSS (Condon et al. 1998) map in Figure 4.

The source-subtracted data were then remapped with a uv-taper of 500 λ to increase the sensitivity to the S–Z effect and are shown in Figure 5. The integrated S–Z flux in the map is -8.61 mJy and the noise on the map
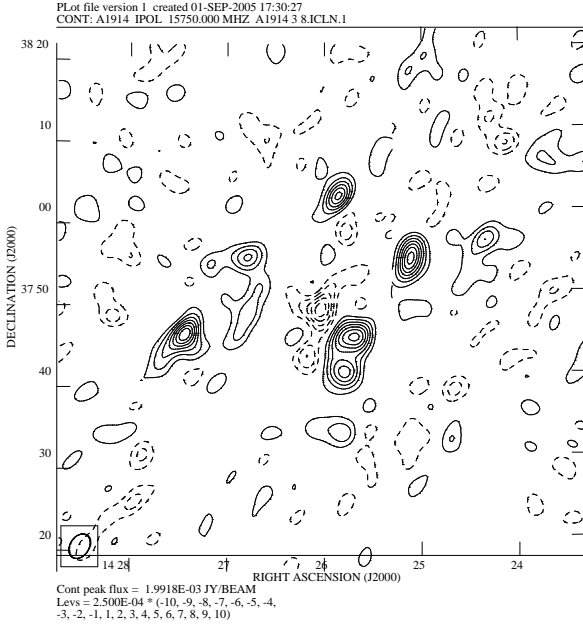
PLot file version 1 created 01-SEP-2005 17:30:27
CONT: A1914 IPOL 15750.000 MHZ A1914 3 8.ICLN.1

Cont peak flux = 1.9918E-03 JY/BEAM
Levs = 2.500E-04 * (-10, -9, -8, -7, -6, -5, -4,
-3, -2, -1, 1, 2, 3, 4, 5, 6, 7, 8, 9, 10)

Figure 2. Naturally weighted, CLEANed AMI map of the A1914 field before source subtraction. The noise on the map is 0.15 mJy/beam.

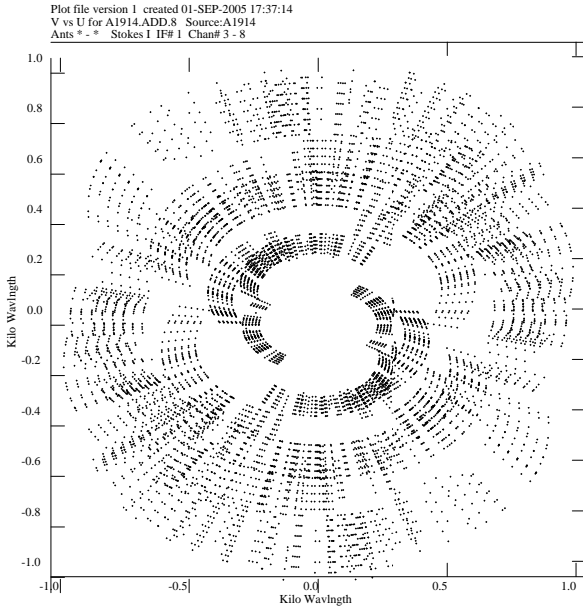Plot file version 1 created 01-SEP-2005 17:37:14
V vs U for A1914.ADD.8 Source:A1914
Ants * - * Stokes I IF# 1 Chan# 3 - 8

Figure 3. Aperture plane coverage for the six channels used.

Table 1. Sources subtracted from the S–Z map. The flux densities are those subtracted from the visibilities, i.e. not corrected for the primary beam.

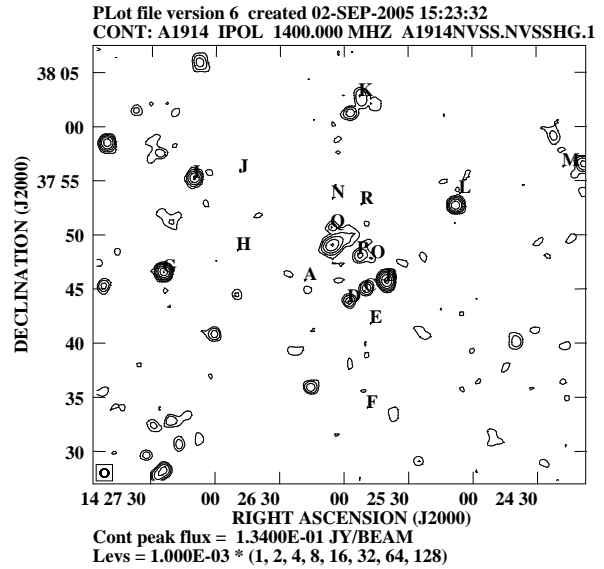| Source	RA (J2000)	Dec. (J2000)	Flux density (mJy)
A	14 26 18.60	+37 45 51.0	0.70
B	14 25 40.70	+37 45 46.4	1.90
C	14 25 50.80	+37 44 51.0	0.65
D	14 25 58.40	+37 43 51.0	0.65
E	14 25 48.00	+37 41 51.0	1.4
F	14 25 49.50	+37 34 06.0	1.02
G	14 27 24.82	+37 46 33.1	1.91
H	14 26 50.20	+37 48 35.0	0.82
I	14 27 10.53	+37 55 14.0	0.32
J	14 26 49.10	+37 55 50.2	0.91
K	14 25 53.30	+38 02 51.0	1.6
L	14 25 06.40	+37 53 50.0	2.1
M	14 24 18.00	+37 56 18.0	1.05
N	14 26 06.00	+37 53 21.0	0.84
O	14 25 47.60	+37 47 48.8	0.54
P	14 25 54.00	+37 48 13.1	0.24
Q	14 26 06.50	+37 50 41.6	0.20
R	14 25 52.60	+37 52 49.0	0.52

PLot file version 6 created 02-SEP-2005 15:23:32
CONT: A1914 IPOL 1400.000 MHZ A1914NVSS.NVSSHG.1

Cont peak flux = 1.3400E-01 JY/BEAM
Levs = 1.000E-03 * (1, 2, 4, 8, 16, 32, 64, 128)

Figure 4. NVSS map of the A1914 field indicating the positions of the 18 sources subtracted from the AMI data.

5 DISCUSSION

The S–Z effect is detected with extremely high significance (Figure 5) and extended structure is clearly visible. Comparing the map from 34 hours of AMI observation with the previous RT map demonstrates the potential of AMI as a cluster survey instrument. Maps of short observations that are limited by thermal noise show that the Small Array sensitivity per channel is approximately 350 mJy s$^{-1/2}$, which is consistent with that assumed in our simulations (Kneissl et al. 2001). Calculations based on the 9C survey source counts (Waldram et al. 2003) show that the AMI maps presented here are limited by source confusion (Scheuer 1957) rather than thermal noise. This and the fact that we have had to remove 18 point sources from our
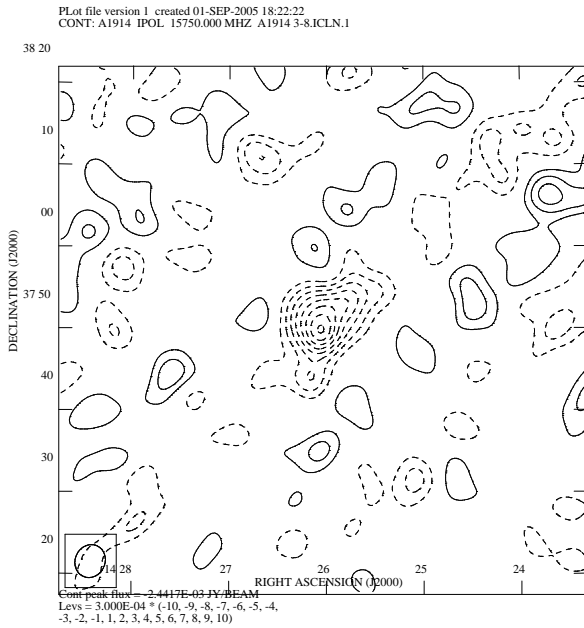
is 0.19 mJy/beam. It is also possible to make maps of individual frequency channels and use these to measure the frequency spectrum of the S–Z effect. Since the S–Z effect is extended and the aperture plane coverage for each channel is different (and hence samples different angular scales), it is necessary to measure the flux from each of the channels over the same solid angle. Figure 6 shows the integrated S–Z flux density over a 56-square-arcminute region at the cluster centre against channel centre frequency.

PLot file version 1 created 01-SEP-2005 18:22:22
CONT: A1914 IPOL 15750.000 MHZ A1914 3-8.ICLN.1

Cont peak flux = -2.4417E-03 JY/BEAM
Levs = 3.000E-04 * (-10, -9, -8, -7, -6, -5, -4,
-3, -2, -1, 1, 2, 3, 4, 5, 6, 7, 8, 9, 10)

Figure 5. CLEANed map of the S–Z effect in A1914 after source subtraction and with a *uv*-taper of 500 λ, resulting in a resolution of $247 \times 216''$. The noise on the map is 0.19 mJy/beam. The S–Z effect is clearly resolved and has an integrated flux density of -8.61 mJy.
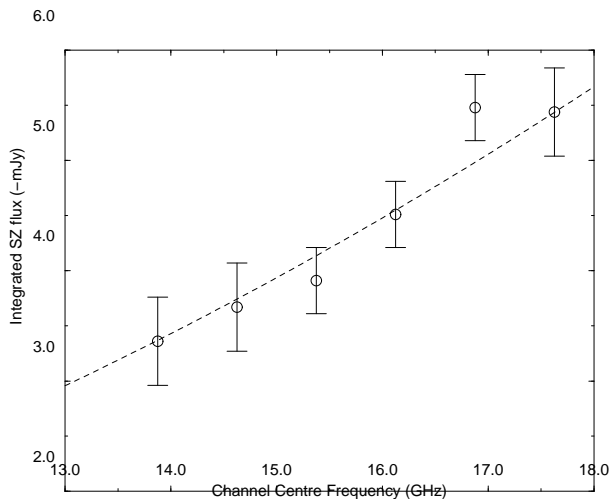

Figure 6. Spectrum of the S–Z effect in A1914. The integrated flux is found over a 56 square arcminute region at the cluster centre. The magnitude of the negative S–Z flux is shown for convenience. The error bars are the 1σ errors from the channel maps which are dominated by source confusion; errors between different channels are therefore not independent. The dashed line shows a thermal spectrum ($\alpha = -2$ in the Rayleigh-Jeans region) constrained to pass through the 13.875 GHz point.

data emphasise the importance of source subtraction, which for AMI will be provided by the Large Array.

Figure 6 shows that the spectrum of the decrement measured by AMI is consistent with an S–Z spectrum, which differs from a thermal spectrum by less than 0.5% between 13.5 and 18 GHz (Challinor & Lasenby 1998).

In order to make a preliminary comparison of the AMI data on A1914 with X-ray observations, we have fitted an isothermal spherical β-model, assuming a concordance cosmology ($H_0 = 72 \, \mathrm{km \, s^{-1} \, Mpc^{-1}}$, $\Omega_M = 0.3$, $\Omega_\Lambda = 0.7$), to Chandra ACIS-I data using a temperature $T = 8.41 \, \mathrm{keV}$ (Ikebe et al. I2002), redshift $z = 0.1712$, a count rate calculated from NORAS PSPC and n_H using the HEASARC webPIMMS tool with a Raymond Smith profile (Böhringer et al. 2000). We find best fit parameters of $\beta = 0.731$, central cluster density $n_0 = 0.01627 \, \mathrm{cm^{-3}}$ and core radius $\theta_c = 51.0''$. Using this parameterisation of the intracluster gas, we produce a simulated S–Z observation of the cluster following Grainge et al. (2002). We map and CLEAN this simulated data set in the same manner as the real data and find that the predicted integrated S–Z flux from the X-ray model is -7.35 mJy. This is in good agreement with the value of -8.61 mJy given the assumptions implicit in the model (e.g. that the line of sight depth through the cluster equals the size of the cluster projected on the sky). A more sophisticated simulation of the intracluster gas is beyond the scope of this paper.

The AMI data discussed in this paper come from a commissioning run; further system improvements, such as weighting for system temperature variations through synchronous measurement of injected noise, are underway.

REFERENCES

Baars J. W. M., Genzel R., Pauliny-Toth I. I. K., Witzel A., 1977, A&A, 61, 99

Birkinshaw M., 1999, Phys. Rep., 310, 97

Birkinshaw M., Hughes J. P., ApJ, 1994, 420, 33

Böhringer H., Voges W., Huchra J. P., McLean B., Giacconi R., Rosati P., Burg R., Mader J., Schuecker P., Simiç D., Komossa S., Reiprich T. H., Retzlaff J., and Trümper J., 2000, ApJS, 129, 435

Carlstrom J. E., Holder G. P., & Reese E. D. 2002, ARA&A, 40, 643

Challinor A., Lasenby A. N., 1998, ApJ, 499, 1

Condon J. J., Cotton W. D., Greisen E. W., Yin Q. F., Perley R. A., Taylor G. B., Broderick J. J., 1998, AJ, 115, 1693

Ebeling H., Edge A. C., Böhringer H., Allen S. W., Crawford C. S., Fabian A. C., Voges W. and Huchra J. P, MNRAS, 1998, 301, 881

Grainge K., Jones M. E., Pooley G. G., Saunders R., Edge A., MNRAS, 1993, 265, L57

Grainge K., Jones M. E., Pooley G. G., Saunders R., Baker J., Haynes T., Edge A., 1996, MNRAS, 278, L17

Grainge K., Jones M. E., Pooley G. G., Saunders R., Edge A., Grainger, W. F., Kneissl, R., 2002, MNRAS, 333, 318

Grego L., Carlstrom J. E., Reese E. D., Holder G. P., Holzapfel W. L., Joy M. K., Mohr J. J. and Patel S., 2001, ApJ, 552, 2

Holzapfel W.L. et al., ApJ, 481, 35

Ikebe Y., Reiprich T.H., Bohringer H., Tanaka Y., Kitayama T. 2002 A&A 383, 773

Jones M. E., 2002, ASPC, 257 in 'AMiBA 2001: High-z Clusters, Missing Baryons, and CMB Polarization', edited by Lin-Wen Chen, Chung-Pei Ma, Kin-Wang Ng, and Ue-Li Pen., ASPC, San Fransisco, 257, 35

Jones M. E., Edge A. C., Grainge K., Grainger, W. F., Kneissl R., Pooley G. G., Saunders R., Miyoshi S. J., Tsuruta T., Yamashita K., Tawara Y., Furuzawa A., Harada A. and Hatsukade I., 2005, MNRAS, 357, 518

Kneissl R., Jones M., Saunders R., Eke V., Lasenby A., Grainge K., Cotter G., 2001, MNRAS, 328, 783

Komatsu E. et al., 1999, ApJ, 516, L1

Kosowsky A., 2003, NewAR, 47, 939

Lancaster K. et al., 2005, MNRAS, 359, 16

Lo K., 2002, in 'AMiBA 2001: High-z Clusters, Missing Baryons, and CMB Polarization', edited by Lin-Wen Chen, Chung-Pei Ma, Kin-Wang Ng, and Ue-Li Pen. ASPC, San Francisco, 257, 3

Holder G. P., Mohr J. J., Carlstrom J. E., Evrard A. E., Leitch E. M., 2000, ApJ, 544, 629

Mohr J.J. et al, 2003, NuPhS, 124, 63

Myers S. T., Baker J. E., Readhead A. C. S., Leitch E. M., & Herbig, T. 1997, ApJ, 485, 1

Pointecouteau E. et al., ApJ, 519, L115

Reese E. D., Mohr J. J., Carlstrom J. E., Joy M., Grego L., Holder G. P., Holzapfel W. L., Hughes J. P., Patel S. K., Donahue M., ApJ, 2000, 533, 38

Scheuer P. A. G., 1957, PCPS, 53, 764

Sunyaev R. A., Zel'dovich Ya B., 1972, Comm. Astrophys. Sp. Phys., 4, 173

Udomprasert P. S., Mason B. S., Readhead A. C. S., Pearson T. J., 2004, ApJ, 615, 63

Waldram E. M., Pooley G. G., Grainge K. J. B., Jones M. E., Saunders R. D. E., Scott P. F., Taylor A. C., 2003, MNRAS, 342, 915